

Use of a multi-tube Nafion[®] membrane dryer for
desolvation with thermospray sample introduction to
inductively coupled plasma-atomic emission
spectrometry

by J. Yang, T. Conner, J. Koropchak, D. Leighty



ELSEVIER

Spectrochimica Acta Part B 51 (1996) 1491–1503

SPECTROCHIMICA
ACTA
PART B

Use of a multi-tube Nafion® membrane dryer for desolvation with thermospray sample introduction to inductively coupled plasma-atomic emission spectrometry

Jinfu Yang^a, Timothy S. Conner^a, John A. Koropchak^{a,*}, David A. Leighty^b

^a*Department of Chemistry and Biochemistry, Southern Illinois University at Carbondale, Carbondale, IL 62901, USA*

^b*Perma Pure Inc., 8 Executive Drive, Toms River, NJ 08754, USA*

Received 22 January 1996; accepted 25 March 1996

Abstract

A multi-tube Nafion® membrane dryer used as a part of a desolvation system in conjunction with thermospray nebulization was optimized and characterized with inductively coupled plasma-atomic emission spectrometry (ICP-AES). Either argon or nitrogen could be used as the sweep gas, and optimum conditions were found to be at low temperature and low sweep gas flow rate. Analyte sensitivity was not significantly affected by placing the membrane between the plasma and the nebulizer, although about 20% of the analyte entering the dryer is lost within the dryer. A dual role of the membrane dryer was demonstrated. As a secondary step within the desolvation system, it enabled a high desolvation efficiency of 99.94% for aerosols from 1% (v/v) nitric acid. Plasma solvent load could be reduced to 0.9 mg min⁻¹ with a tap water cooled condenser combined with the membrane dryer, compared to 21 mg min⁻¹ with the normal chilled condenser desolvation system. Meanwhile, the membrane was also found to act as a pulse dampener, eliminating the plasma pulsation in the central channel caused by thermospray nebulization and thus improving the analytical performance of the system. The average relative standard deviations (RSD) with the optimized membrane/thermospray system were 0.83% and 0.60% for the background and analyte signals, respectively, which were reduced by a factor of 1.9 and 2.7 for the background and analyte signals, respectively, compared to thermospray without the membrane desolvation, and were essentially identical to those obtained with pneumatic nebulization sample introduction. The improvements in detection limits with the membrane/thermospray system were 1.2–3.0 times with an average factor of 1.8 compared to thermospray without the membrane dryer, and 18–68 times with an average factor of 39 compared to the standard pneumatic nebulization sample introduction system without a desolvation unit. The detection limits for Mn, Mg, Cr and Cd with the present thermospray/membrane system were comparable to those reported for pneumatic nebulization ICP mass spectrometry.

Keywords: Aerosol desolvation; Desolvation; Inductively coupled plasma-atomic emission spectrometry; Nafion® gas dryer; Non-porous membrane; Thermospray nebulization

1. Introduction

Samples are mostly introduced into an inductively

coupled plasma (ICP) as aqueous aerosols. It has been shown that the introduction of water influences the excitation conditions and analytical performance of the plasma [1–8]. In the presence of water as aerosol, the plasma visually contracts in size and moves up

* Corresponding author.

relative to the top of the torch, and the central channel becomes much more pronounced [1,2]. Aerosol droplets travel a substantial distance up the central channel before all of the solvent is removed, resulting in a delayed onset of excitation, and thus peak emission intensities for analytes occur higher in the plasma [3]. Olesik et al. [4] reported experimental evidence of intact droplets at heights up to 20 mm above the load coil in a 1 kW ICP. The droplets have a large effect on local plasma conditions and cause large fluctuations in emission intensities. While some workers [1,5,6] observed decreases in excitation temperature, ionization temperature and electron density when water was removed, others [7,8] reported opposite results. Long and Browner [2] observed that there is a difference between the interaction of water vapor and water aerosol with an ICP. Water introduced as aerosol greatly increases the noise level in background intensity and decreases ionization temperature and electron density, whereas water present as vapor alone has small effects.

Acidic solutions are widely used in ICP atomic spectrometry. Recent studies showed that introduction of mineral acids into ICP results in decreases in excitation temperature and exerts depressive effects on analyte intensity because of a decrease in the energy transfer from the plasma to the analytes [9–11]. In addition, the introduction of water and acid adds to the complexity of plasma background spectra. Overall, Browner et al. [12] concluded that an ideal sample introduction system for ICP spectrometry would have a high analyte transport rate and a low solvent transport rate.

Pneumatic nebulization (PN) is the most common means of aerosol generation for ICP spectrometry. However, sample introduction with pneumatic nebulization is highly inefficient (typically about 1%) at typical sample flow rates ($1\text{--}2\text{ ml min}^{-1}$). While low efficiency implies low solvent transport, it also means low analyte mass flux into the plasma, and the potential capabilities of ICP spectrometry are thus substantially limited with pneumatic nebulization sample introduction. Many attempts have been made to develop high performance sample introduction systems for ICP. These include the use of ultrasonic nebulization [13], hydraulic high pressure nebulization [14,15] and thermospray nebulization [16]. These sample introduction systems significantly

improve the detection limits obtainable with ICP-AES, primarily through increases in analyte transport. However, the enhanced performance could be achieved only after a substantial reduction of solvent loading to the plasma [14,15,17]. When excessive solvent enters the plasma, the rate of increase of signal with increasing analyte mass flux is reduced, and/or the plasma becomes unstable or even extinguished. Therefore, a high performance sample introduction system must be used in conjunction with a desolvation device.

A conventional desolvation system is comprised a heated spray chamber and a condenser. The latter is commonly cooled by a refrigerated recirculating bath that is relatively expensive. Peltier coolers [14,18] and cryogenic condensers [19–21] are also employed to condense the solvent vapors from the heated spray chamber. While the use of these systems does not reduce costs, detection limits were reported to be degraded with cryogenic desolvation [22]. One potential disadvantage to low temperature vapor removal is that condensation can not only occur on the condenser surface, but also back onto analyte particles in the aerosol phase, limiting the efficiency of solvent removal, leaving solvent in the less desirable aerosol phase and possibly leading to loss of analyte [23]. This process undoubtedly led to the requirement for repeated heating and cooling steps for most efficient solvent removal with cryogenic desolvation [21].

Recently, removal of solvent with membrane separators has been described [22,24–27]. This seems a promising type of desolvation and has been of particular interest. One such device is Vestec's universal interface, originally developed for liquid chromatography mass spectrometry [28], and another is Cetac's MDX-100 membrane desolvator for ultrasonic nebulization [29], both of which are commercially available. In these systems, a porous membrane is used, through which solvent vapor diffuses to the waste while the relatively large, dry analyte particles remain inside the membrane tube and are swept into the ICP. The sweep gas must be the same as the plasma gas and the membrane needs to be operated at elevated temperature to speed up the diffusion of solvent vapors.

In the present work we will describe the optimization and characterization of a Nafion® membrane dryer when used for desolvation with thermospray

sample introduction to ICP-AES. Nafion® is a polymer similar to Teflon except that a sulfonic acid group is added to the chain giving the material a high affinity for water. The Nafion® membrane is nonporous, and water removal is based on absorption and desorption processes, which give an opportunity to use a sweep gas different from the plasma gas and eliminate problems of flow balance inside and outside the membrane. Successful applications of Nafion® dryers to moisture removal in chemical vapor generation atomic spectrometry have been reported [30–32], and our recent studies [33] on the use of a single tube Nafion® dryer in ICP-AES also showed promising results. The Nafion® dryer used in this study consists of an array of 200 microtubular membranes, providing very high surface areas for solvent absorption and desorption. The analytical figures of merit of the thermospray/membrane ICP-AES system and the fundamental performance of the membrane for solvent removal and analyte transport will be described

with both argon and nitrogen as the sweep gas for the membrane. Further, we will discuss the action of the multi-tube membrane system as a gas-phase pulse dampener to counteract pulsation, known to limit measurement precision with thermospray sample introduction and 40 MHz ICP-AES [34].

2. Experimental

2.1. ICP spectrometer and operating conditions

All spectroscopic measurements were performed using a Varian Liberty 220 ICP spectrometer (Victoria, Australia), consisting of a plasma source powered by a crystal-controlled high frequency generator operating at 40.68 MHz and a vacuum path monochromator with a Czerny-Turner mount. The spectrometer has a resolution of 18 pm for the first order and 6 pm for the fourth order. All data were collected at an

Table 1
Experimental conditions

Analytical Wavelengths Element	Order	Thermospray		Pneumatic	
		Wavelength/nm	Atom (I)/Ion (II)	Wavelength/nm	Atom (I)/Ion (II)
Tl	1st	190.7	I	1.25	I
As	1st	193.6	I	15.0	I
Se	1st	196.0	I	1.5	I
Ni	2nd	231.6	II	0.70	II
Mn	2nd	257.6	II	7	II
Mg	2nd	279.5	II	1.5	II
Cu	2nd	324.7	II	195°C	II
Pb	3rd	220.3	II	150°C	II
Cd	3rd	228.8	I	25°C when the membrane was used	I
Cr	2nd	267.7	II	–7°C when the membrane was not used	II

integration time of 5 s with 5 replicates for standards and 10 replicates for blanks. Detection limits were calculated as the concentration giving a signal equal to three times the standard deviation of the blank, based on 10 replicate measurements. For the collection of detection limit data with pneumatic nebulization (PN), a type K concentric nebulizer (Glass Expansion, Australia) was used with the standard Varian Sturmman-Masters spray chamber. The standard pressure regulator was used to control the nebulizer gas flow rate with PN and the optimum pressure is reported in Table 1. For all other experiments, a thermospray nebulizer was employed. A Mn solution was used to establish the compromise plasma conditions. The final optimized conditions, which are based on obtaining maximum signal-to-background ratios and minimum relative standard deviations for Mn at 257.6 nm, and analytical wavelengths are listed in Table 1.

2.2. Thermospray nebulizer and desolvator

The sample introduction system is shown in Fig. 1. A fused silica aperture thermospray nebulizer, details of which have been previously described [35], was

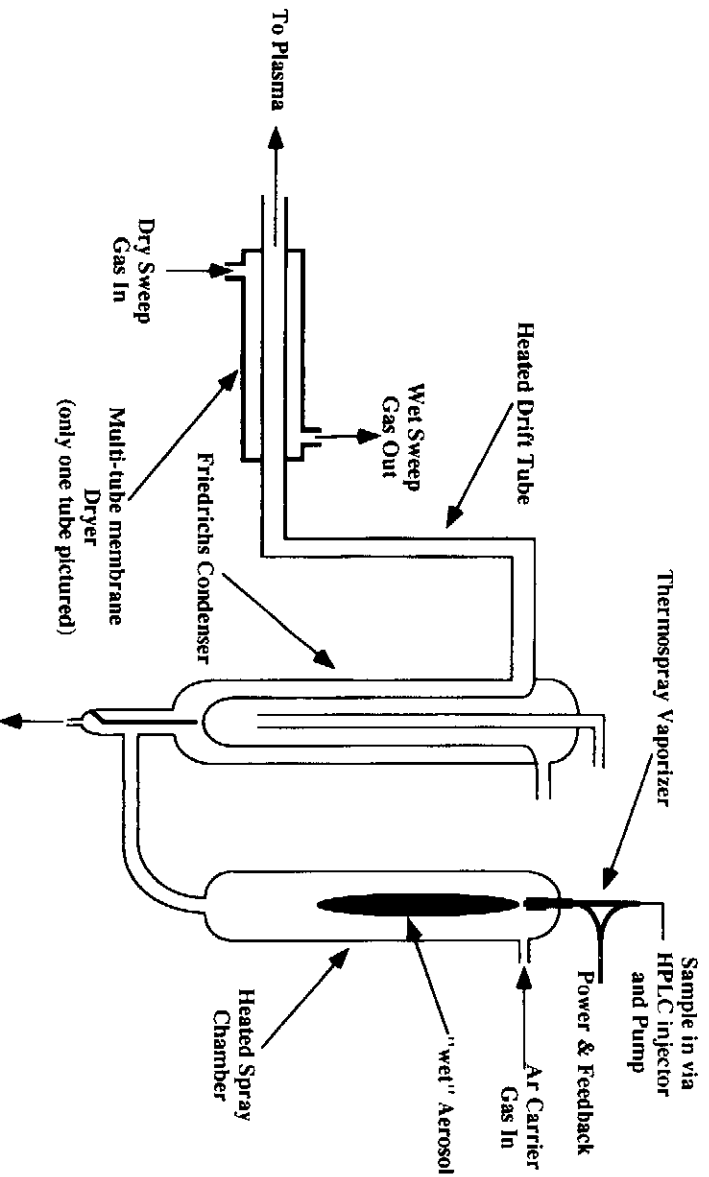


Fig. 1. Diagram of the sample introduction system used in this work.

used for aerosol generation. Based on the previous work [35], the solution flow rate of 1.5 ml min⁻¹ was used. The optimal control temperature and spray chamber temperature were found to be 195 and 150°C, respectively (Table 1). The particular thermospray system used herein was a prototype constructed by Leeman Labs, Inc. This system employs a standard fused silica aperture thermospray nebulizer and glassware arrangement as described by Koropchak et al. [35], but uses digital controllers to monitor and control the operating temperatures versus the analog triac controllers used in the past publications. Specifically, two CN 9000A digital temperature controllers from Omega Engineering, Inc. (Stamford, CT, USA) were used to monitor and regulate the control and spray chamber temperatures. An Autochrom (Berlin, Germany) model M500 HPLC pump continuously delivered a carrier flow of 1% (v/v) nitric acid in distilled deionized water to the nebulizer, and sample solutions containing 1% (v/v) nitric acid were introduced in flow injection manner with a Rheodyne (Cotati, CA) model 7125 metal free injector fitted with a 20 ml PEEK injection loop followed by a 2 µm particle filter. Finally, the Ar carrier gas flow rate was

monitored and controlled using a mass flow controller (model FC-260, Tylan General, Torrance, CA).

Therospray aerosols were input into a cylindrical Pyrex spray glass chamber heated to 150°C. High efficiency desolvation of the aerosol was accomplished by the combination of a Friedrichs condenser (maintained to 25°C with tap water) followed by a Nafion® membrane dryer. A Pyrex glass drift tube, 50 cm in length and 15 mm inner diameter, was used to connect the outlet of the condenser and the inlet of the membrane. To prevent the residual solvent in the aerosol stream from condensing onto particles, the drift tube was heated to 85°C using a heating tape. The temperature was controlled with a variable AC power supply and monitored with a J type thermocouple thermometer (model 600–2720, Barnant Company, Barrington, IL, USA). The dry aerosol from the membrane was introduced into the ICP. When the membrane was not used, the Friedrichs condenser was cooled to –7°C. The condenser temperature was regulated using a refrigerated-recirculating bath (NESLAB Instruments, Inc., Newington, NH, USA).

A Model PD-1000 Nafion® membrane dryer (Perma Pure, Inc., Toms River, NJ, USA), composed of 200 tubes each with an internal diameter of 0.6 mm and a wall thickness of 0.1 mm, was used in this study.

The tubes are held together with a common epoxy resin header and housed in a stainless steel shell with 2.2 cm internal diameter. The dryer has a length of 60 cm and an internal surface area of 2300 cm².

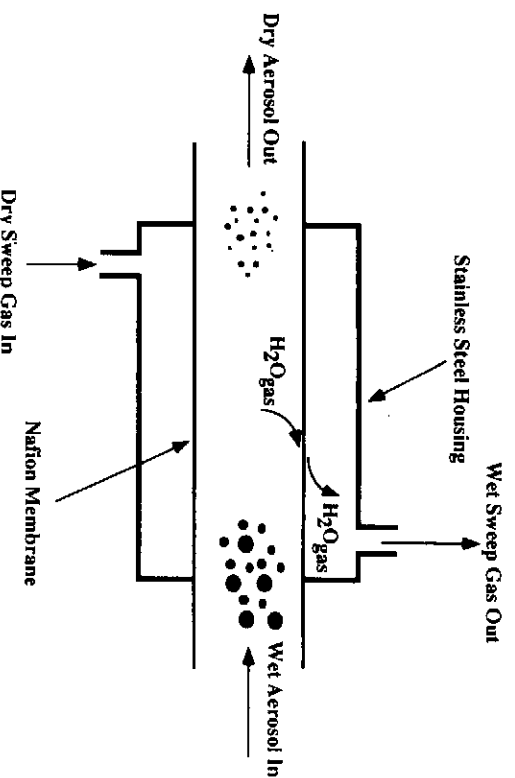


Fig. 2. Illustration of the drying principle with a single tube Nafion® membrane dryer.

This is about 20 times more surface area than the single-tube membrane dryer reported in the previous work [33]. The principle of drying with the Nafion® dryer is shown in Fig. 2 for one of the 200 microtubes. When a wet gas stream flows through the tubes, water vapor molecules are adsorbed by the highly hygroscopic membrane. Driven by the concentration gradient, the adsorbed water moves through the wall of the tubing, desorbing to the external countercurrent sweep gas passing around the outside of the tubes. Unless stated otherwise, 2 l min⁻¹ of nitrogen was used as the sweep gas. The first 30 cm of the dryer was placed in a electrically heated steel block. Temperature control was accomplished with a CAL 3200 (CAL Controls Ltd, Libertyville, IL, USA) autotuning temperature controller; temperature feedback was provided by a J type thermocouple placed in the outlet of the sweep gas for the membrane. The sweep gas outlet temperature was maintained at 35°C to prevent condensation at the aerosol entrance.

This membrane system has been used for desolvation of aqueous and organic (methanol) aerosols for 7 months without any degradation in performance or operation.

2.3. Analyte and solvent transport measurement

The procedure used for analyte transport measurements was similar to that described previously [17,36]. Solutions containing 50 µg ml⁻¹ of the

analytes in 1% (v/v) nitric acid solutions were nebulized by the thermospray nebulizer. Aerosols exiting from an aerosol injection tube connected to the outlet of the Friedrichs condenser or the membrane dryer were collected on glass microfibre filters (Whatman EPM 2000, Whatman International Ltd., Maidstone, UK) fixed by a Teflon® filter holder. An excess of gas was drawn through the filters by an external vacuum source. The aerosol injection tube was placed inside a larger diameter sampling tube connected to the filter holder to minimize the effects of the vacuum on aerosol transport. The collected aerosol was then leached from the filters with 1% (v/v) nitric acid and an ultrasonic bath, and transferred into volumetric flasks. The solutions were analyzed with the same Varian ICP-AES spectrometer but using the pneumatic nebulizer mentioned above. The results provided a direct measure of analyte transport. A mass balance was also checked by separately rinsing the spray chamber and the condenser and collecting the nontransported analytes.

Desolvation efficiency measurements were performed for 1% (v/v) HNO_3 or pure water without analytes added using a solvent trap composed of two silica gel packed U-tubes connected in series and by weighing the trapped amount of solvent [2,12]. The mass of solvent collected on the second trap was always found to be negligible compared to that collected on the first, indicating the nearly complete collection of the solvent by the first silica gel trap. In order to achieve acceptable precision with the analytical balance, a minimum of 100 mg of water was collected. To get this desired level of precision, the collection times were varied from 30 min when no membrane desolvator was used, to 230 min when the membrane desolvator was used.

3. Results and discussion

3.1. Optimization of membrane temperature

Here the term 'membrane temperature' refers to the temperature of the sweep gas measured at the outlet from the membrane. Fig. 3 and Fig. 4 show the effects of membrane temperature at the sweep argon flow rate of 6.1 min^{-1} . Analyte sensitivities for all the elements tested decreased somewhat as membrane temperature

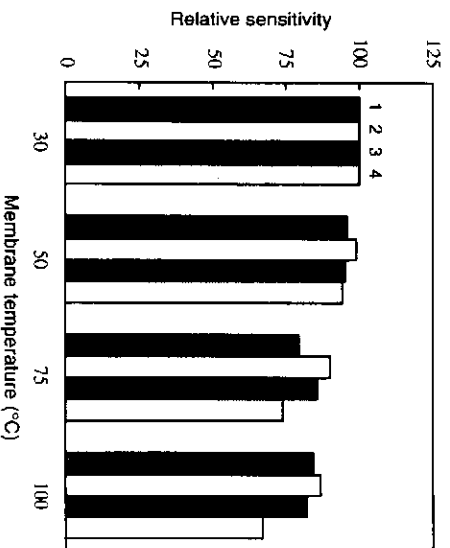


Fig. 3. Effect of membrane temperature on analyte sensitivity at the sweep argon flow rate of 6.1 min^{-1} . The sensitivity at 30°C was set to 100 and all the measurements were ratioed to it. 1:As, 2:Cr, 3:Cu and 4:Pb.

increased from 30 to 100°C (Fig. 3). The dependence of background intensity on membrane temperature has two types of trends (Fig. 4). Background intensities at TI 190.7 nm , As 193.6 nm and Se 196.0 nm significantly increase with increasing membrane temperature, whereas those at the other analyte wavelengths remain unchanged in the temperature range from 30 to 100°C . Spectral scans in a window of

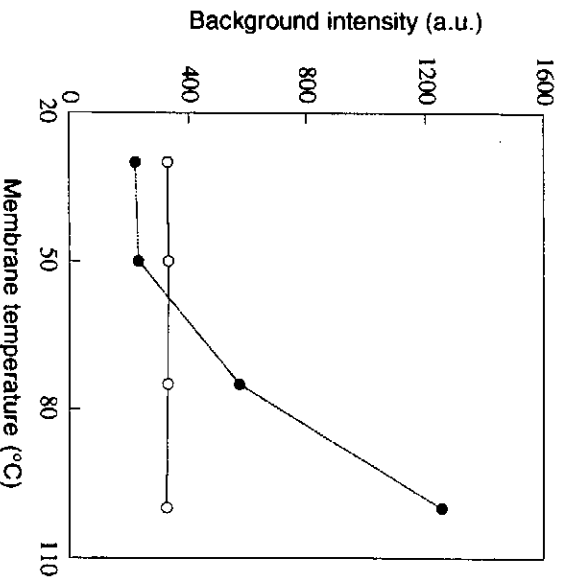


Fig. 4. Effect of membrane temperature on background intensity for As (●) and Pb (○) at the sweep argon flow rate of 6.1 min^{-1} .

110 pm centered on an analyte line revealed the appearance of extra structure in the spectral background around Se 196.0 nm at the high membrane temperature of 100°C, suggesting that the increased background intensity at these wavelengths is probably due to molecular bands resulting from the introduction of some membrane and/or fitting materials into the carrier gas. From both Fig. 3 and Fig. 4, it seems that 50°C is a critical temperature below which the membrane temperature has little effect on either analyte sensitivity or background intensity. Overall, it is satisfactory to keep the membrane at the lowest temperature possible without condensing the solvent to obtain maximum signal-to-background ratios and desolvation efficiency. The membrane contains adsorbed water, and the vapor pressure of water adsorbed to the membrane is positively proportional to its temperature. As temperature increases, the amount of adsorbed water increases and the final water content of the sample consequently also increases. Therefore, a lower membrane temperature will produce a higher water vapor reduction and consequently a higher desolvation efficiency. In this work, the membrane temperature of 35°C was selected, at which the membrane could be continuously operated for a long period (e.g. 10 h) without any solvent condensation in the membrane. It should be noted that condensation of solvent onto the membrane largely renders the membrane inactive to vapor removal, and is therefore undesirable.

3.2. Effect of sweep gas flow and composition

The sweep gas is another adjustable parameter with the membrane desolvator. Theoretically, a non-porous membrane desolvator should offer more flexibility in the selection of sweep gas and its flow rate than a porous membrane desolvator. Argon and nitrogen were tested in this study. The effect of argon sweep flow rate on As, Cr, Cu and Pb is shown in Fig. 5. It can be seen from Fig. 5(a) that at an Ar flow rate above 6 l min⁻¹, the sensitivities for As, Cr and Pb decrease with an increase in Ar flow rate while that for Cu increases somewhat. The behavior for Tl, Mn, Mg, Ni and Cd was the same as observed for As, Cr and Pb, whereas the data for Se showed a similar trend with Cu. The background intensities were found to decrease with increasing sweep argon flow rate in a

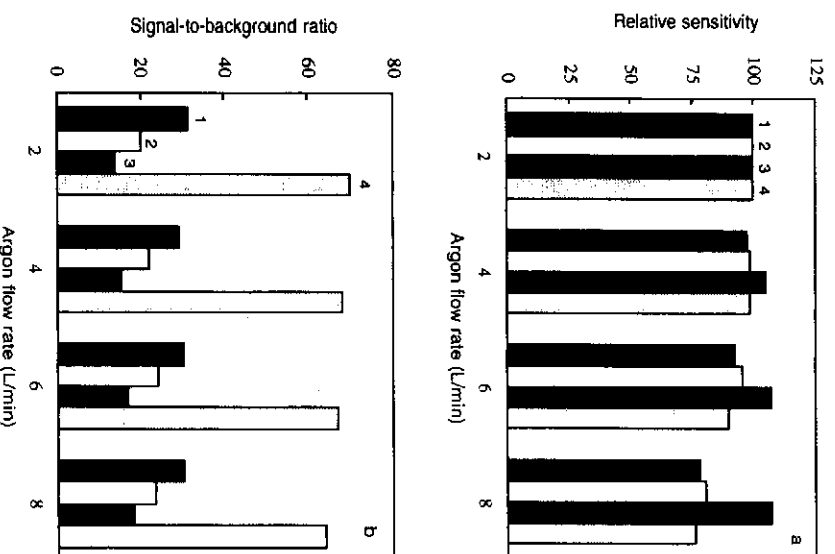


Fig. 5. Dependence of analyte sensitivity (a) and signal-to-background ratio (b) for a solution containing 1 $\mu\text{g ml}^{-1}$ As and Pb and 0.1 $\mu\text{g ml}^{-1}$ Cr and Cu on sweep argon flow rate. For (a) the sensitivity at the sweep argon flow of 2 l min⁻¹ was set to 100 and all the measurements were ratioed to it. 1:As, 2:Cr, 3:Cu and 4:Pb.

similar way for all the analytes. A possible reason for these observations is a transfer of a small portion of the sweep gas at a high flow rate into the aerosol stream, which increases the actual flow rate of the carrier gas and eventually results in changes in background and analyte signal. The mechanism of the transfer of the sweep gas across the membrane is not clear but Nafion® membranes, in spite of their non-porous property, do have very small permeability for non-polar gases such as N₂, and it is also possible that there is some leakage somewhere in the fittings. The signal-to-background ratios (Fig. 5(b)) and relative standard deviations (RSD) for analyte signal and background intensity (Fig. 6) are largely unchanged in the tested range of sweep argon flow

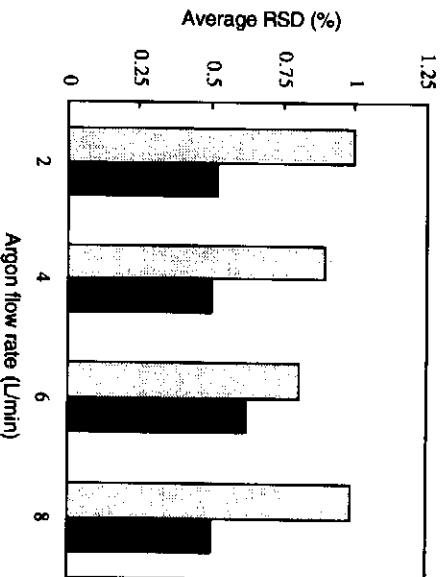


Fig. 6. Dependence of the average relative standard deviations for 10 elements on sweep argon flow rate. Gray bar: background RSD for the 1% (v/v) nitric acid blank solution, black bar: analyte signal RSD for a solution containing $1\mu\text{g ml}^{-1}$ As, M, Se, Ni and Pb and $0.1\mu\text{g ml}^{-1}$ Mn, Mg, Cr, Cd and Cu.

rate, and therefore the analytical performance of the ICP is largely unaffected.

When nitrogen was used as the sweep gas, the central channel of the plasma became larger at a nitrogen flow rate higher than 6 l min^{-1} and a visible pulsation in the central channel occurred. Here again, the observations suggest the transfer of a small portion of the sweep gas across the membrane into the aerosol stream, and the transfer seems to increase with membrane temperature as it was observed that at a membrane temperature of 50°C even a nitrogen flow rate of 4 l min^{-1} caused a visible change in the central channel. The effects of sweep nitrogen flow rate on As, Cr, Cu and Pb are shown in Fig. 7, where all the data with nitrogen as the sweep gas were normalized to those obtained with 6 l min^{-1} sweep argon flow rate. It can be clearly seen that the use of nitrogen as the sweep gas a flow rate of $2\text{--}4\text{ l min}^{-1}$ does not result in a significant decrease in sensitivity and signal-to-background ratio compared with argon as the sweep gas. However, unlike the case for argon as the sweep gas (Fig. 5), both analyte sensitivity and background intensity significantly decrease with an increase in nitrogen flow rate (only sensitivity data being shown in Fig. 7). As a result the optimal sweep nitrogen flow rate for optimal signal-to-background ratio varies from element to element (Fig. 7(b)). More importantly the plasma pulsation due to the introduction of some

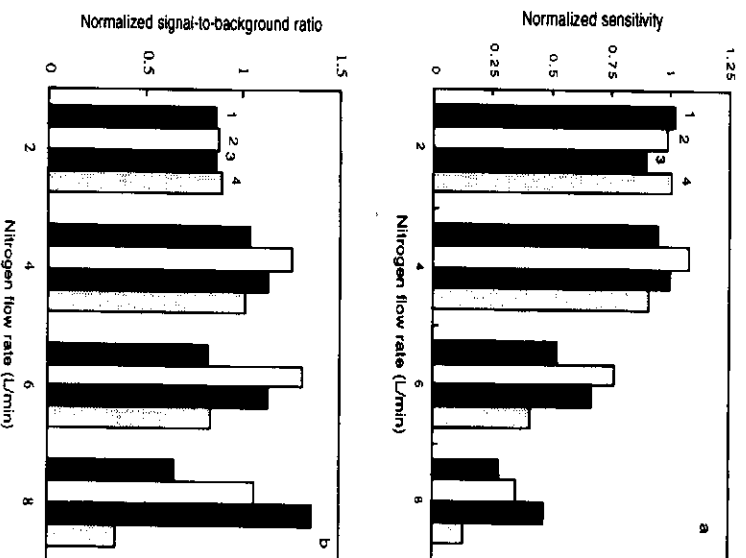


Fig. 7. Dependence of analyte sensitivity (a) and signal-to-background ratio (b) for a solution containing $1\mu\text{g ml}^{-1}$ As and Pb and $0.1\mu\text{g ml}^{-1}$ Cr and Cu on sweep nitrogen flow rate. All the data were normalized to those obtained with 6 l min^{-1} sweep argon flow rate. 1:As, 2:Cr, 3:Cu and 4:Pb.

nitrogen at a flow rate equal to or higher than 6 l min^{-1} caused increased relative standard deviations (RSD) up to about 2.5% for both analyte signal and background intensity (Fig. 8). The effect of the pulsation on RSDs for analyte signal is larger than on RSDs for background, which can be understood by the fact that the pulsation happens in the central channel of the ICP where analyte undergoes excitation and emission, whereas background emission is largely from the surrounding part of the plasma which is less affected by the introduction of nitrogen from the sweep gas. Fortunately, both analyte sensitivity and measurement precision are not significantly changed for a sweep nitrogen flow rate below 4 l min^{-1} and are very close to those with sweep argon flows at or below 6 l min^{-1} . Therefore, good analytical performance could also be achieved with nitrogen as sweep gas if the sweep gas flow rate was small and the membrane

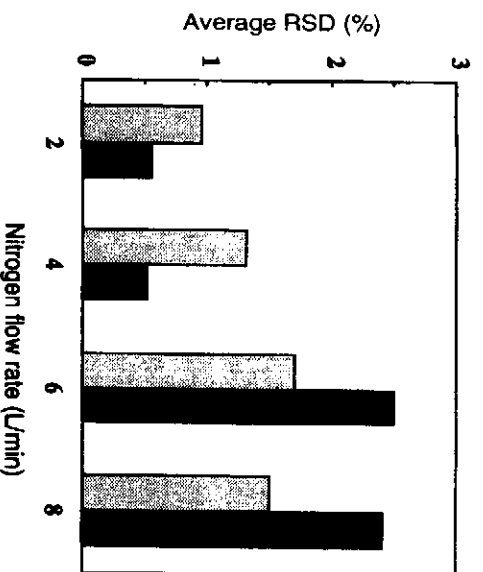


Fig. 8. Dependence of the average relative standard deviations for 10 elements on sweep nitrogen flow rate. Gray bar: background RSD for the 1% (v/v) nitric acid blank solution, black bar: analyte signal RSD for a solution containing $1\mu\text{g ml}^{-1}$ As, Tl, Se, Ni and Pb and $0.1\mu\text{g ml}^{-1}$ Mn, Mg, Cr, Cd and Cu.

temperature was low. The average ratio of detection limits for the 10 elements with 21 min^{-1} sweep nitrogen and 6 l min^{-1} sweep argon is 1.0, indicating no significant difference in detection limits using either nitrogen or argon as the sweep gas.

3.3. Desolvation efficiency

Table 2 lists the desolvation efficiency of the present system for 1% (v/v) nitric acid. Without the membrane and at a condenser temperature of 25°C , the desolvation efficiency is 98.28%. With a decrease of the condenser temperature to -7°C , a limited gain in desolvation efficiency^a was realized. When the membrane dryer is used, however, the desolvation

efficiency is increased up to 99.94%, being significantly higher than the reported desolvation efficiencies in the literature using various types of desolvation systems [14,24,37], and more significantly, the amount of the solvent entering the ICP, shown in the last column of Table 2, is reduced by over a factor of 20, from 21 mg min^{-1} in the absence of the membrane to 0.9 mg min^{-1} when the membrane is used. This large reduction in plasma solvent loading suggests that the use of a Nafion® membrane would be especially beneficial to ICP-MS, where the major oxygen source for oxide interferences is the water in aerosol. It has been suggested that virtually all of the water must be removed in order to lower the oxide levels in ICP-MS [24,25]. With the condenser temperature of -7°C , the actual temperature of the aerosol stream exiting the condenser is about 11°C , at which the theoretical amount of the saturated water vapor in the carrier gas is 7.0 mg min^{-1} . The theoretical value at a condensation temperature of 25° is 16 mg min^{-1} . The measured values are significantly higher than the calculated ones, especially at the lower condenser temperature, indicating a significant amount of water present in the aerosol phase. One cause for this is that the former were obtained with 1% (v/v) nitric acid while the latter were calculated based on pure water. Aerosol particles formed by the trace impurities from nitric acid can act as nuclei sites for condensation of water vapor during the cooling process within the low temperature condenser [23]. A desolvation efficiency of 99.5% was observed for pure water in the absence of membrane and at a condenser temperature of -7°C , at which the amount of water entering the plasma is 7.5 mg min^{-1} , much closer to the amount of the saturated water vapor. Desolvation efficiencies described in the literature for evaluating the performance of a desolvation

Table 2
Solvent transport measurements for 1% (v/v) nitric acid in water (three replicates for each case)

	Desolvation efficiency/% ^a	Amount of solvent entering ICP/(mg min^{-1})
Without membrane, condenser at -7°C	98.59 ± 0.04	21
Without membrane, condenser at 25°C	98.28 ± 0.05	26
With membrane, condenser at 25°C	99.94 ± 0.01	0.90

^a The figures behind \pm are standard deviations; desolvation efficiencies represent the percentage of the introduced solvent (1.5 ml min^{-1}) removed by all mechanisms prior to the ICP.

system were commonly for pure water, which we think does not reflect the real situation. When the membrane dryer was used, we obtained the same desolvation efficiency for pure water as for 1% (v/v) nitric acid, indicating both water vapor and water in the aerosol phase are efficiently removed. This result may also indicate the removal of some portion of the nitric acid through the Nafion® membrane.

3.4. Analyte transport and sensitivity

As listed in Table 3, the transport efficiency, which was essentially the same for all the analytes tested, was measured to be 29% without the membrane. The use of the Nafion® membrane dryer resulted in some loss of analytes and the average analyte transport efficiency for the nine elements decreased to 23%. Because of the non-porous property of the membrane, it is unlikely that analyte particles diffuse through the membrane, and this loss must be due to collection of analyte particles on the membrane. The analyte sensitivity, however, is less affected by the use of the membrane, probably because of an enhanced analyte excitation resulting from lower plasma solvent loading. As shown in Fig. 9, sensitivity ratios with and without the membrane lie between 0.88 and 1.06 for all the analytes except for Tl and Cu, for which the ratios are 0.66 and 0.77, respectively, with an average being 0.9. Compared with pneumatic nebulization, the average sensitivity improvement

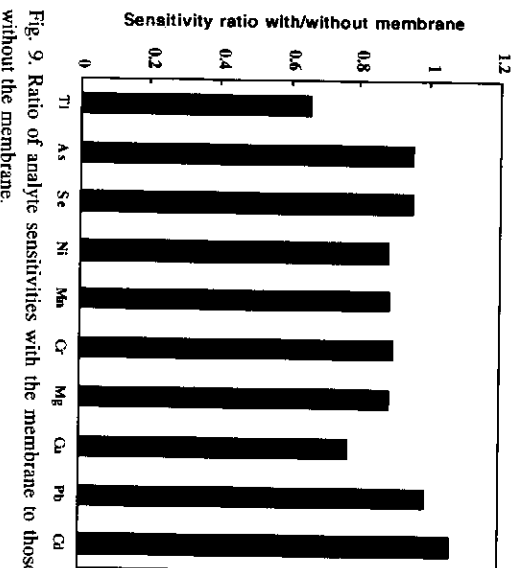


Fig. 9. Ratio of analyte sensitivities with the membrane to those without the membrane.

with thermospray is 43 and 49 times with and without the membrane, respectively. Also listed in Table 3 are measured fractions of analyte collected as waste, showing that about 62% of analyte goes to the drain, 3.7% is collected on the spray chamber and 5.8% on the condenser during nebulization, solvent evaporation and condensation. The average mass balance error was 0.4%.

As indicated earlier, we have operated this desolvation system with the membrane continuously for over 7 months. Although the above data indicated that

Table 3
Analyte transport measurements (three replicates for each case)

	Transport efficiency/ % ^a		Analyte loss/ % ^b			
	No membrane	With membrane	Waste drain	Condenser	Spray chamber	
Tl	28 ± 3	23 ± 1	60.0	3.7	2.5	
As	28 ± 2	22 ± 0.2	62.2	5.5	2.4	
Se	29 ± 2	22 ± 1	63.0	6.7	3.6	
Ni	29 ± 2	23 ± 0.3	62.2	5.8	4.7	
Mn	29 ± 2	23 ± 0.5	62.5	6.0	4.6	
Cr	29 ± 2	23 ± 0.5	62.0	6.1	2.0	
Cu	28 ± 1	22 ± 1	62.5	6.2	4.5	
Pb	29 ± 2	22 ± 0.6	61.9	6.1	4.4	
Cd	29 ± 2	23 ± 0.5	61.1	6.1	4.5	
Average	29	23	61.9	5.8	3.7	

^a The figures behind ± are standard deviations.

^b Obtained using normal thermospray without the membrane dryer.

some analyte is collected on the membrane, we have not observed memory effects on signals resulting from the presence of this analyte. For example, at the end of sample injections baseline signals are achieved within 60–80 s although detailed characterization of washin/washout times have not been conducted. As particle collection on surfaces is generally irreversible within such flow systems, this is not surprising. In the long term, however, it might be expected that collection of such material might influence the performance of the system, and periodic flushing of the membrane with 10% nitric acid and/or other solvents might be required. However, for the period of these studies, no degradation in performance was observed and no cleaning process was employed. Studies of such effects, particularly with higher dissolved solids samples, are currently underway.

3.5. Measurement precision and detection limits

Direct coupling of the thermospray nebulizer with the 40 MHz ICP results in a vertical pulsation in the central channel of the plasma, which significantly deteriorates measurement precision [34] and generally has a larger effect on analyte signal noise than on background noise as explained in the above section. We found that the use of the membrane dryer of this design eliminated the plasma pulsation

and improved measurement precision. As can be seen in Table 4, when the membrane was placed between the thermospray and ICP the RSDs for both analyte signal and background intensity (on average 0.83% and 0.60%, respectively) are comparable to those obtained with pneumatic nebulization. Without the membrane on the other hand, the measurement precision was worse for all the elements and the average RSDs were increased to 1.6% for both background and analyte signal. Further studies [38,39] showed that the noise levels with an unheated spray chamber are lower than those when the spray chamber is heated, suggesting that the plasma pulsation is probably caused by a pressure variation due to the solvent evaporation in the spray chamber. Increasing the back pressure within the sample introduction system by using a torch with a smaller injector [40] and using a latex pulse dampener [38,39] were found to alleviate the symptoms of the plasma pulsation. In this work we demonstrated that the Nafion® membrane dryer of this design can also function for this purpose.

Table 5 compares the detection limits for the different cases. With thermospray nebulization, the use of the membrane dryer results in improved detection limits, on average by a factor of 1.8. Obviously, this improvement is attributed to the reduction of background noise as discussed above. Compared to the standard pneumatic nebulization sample introduction

Table 4
Relative standard deviations (%) for background (RSDB) and signal (RSDS)^a

λ (nm)	Thermospray		No membrane		Pneumatic	
	With membrane		RSDB		RSDB	
	RSDB	RSDS	RSDB	RSDS	RSDB	RSDS
Tl II 190.7	1.9	0.80	3.0	2.1	1.7	2.7
As I 193.6	1.0	0.39	1.7	1.5	1.0	0.92
Se I 196.0	0.64	1.4	1.3	1.0	1.3	0.30
Ni II 231.6	0.58	0.41	1.2	1.4	—	—
Mn II 257.6	0.82	0.32	2.1	2.0	0.37	0.31
Cr II 267.7	0.64	0.17	1.1	2.7	0.44	0.36
Mg II 279.5	0.82	0.33	1.4	1.7	0.53	0.15
Ca I 324.7	0.31	0.65	0.74	0.81	0.29	0.23
Pb II 220.3	1.2	0.94	1.9	1.3	0.75	0.57
Cd I 228.8	0.46	0.57	1.5	1.1	0.60	0.50
Average	0.83	0.60	1.6	1.6	0.78	0.67

^a Calculated from 10 and 5 replicate measurements for background and signal, respectively. A solution with the analyte concentrations of 0.1 $\mu\text{g ml}^{-1}$ for Cu, Cd, Cr, Mn and Mg and of 1 $\mu\text{g ml}^{-1}$ for As, Se, Tl, Pb and Ni was used in the measurement of signal RSDs.

Table 5
Comparison of detection limits (ng ml⁻¹) based on 3σ concept and 10 replicate measurement

λ(nm)	Thermospray		Pneumatic(C)		B/A	C/A
	With membrane(A)	No membrane(B)				
Tl II 190.7	2.5	3.0	170	1.2		68
As I 193.6	1.1	1.6	42	1.5		38
Se I 196.0	1.6	4.8	72	3.0		45
Ni II 231.6	0.13	0.16	—	1.2		—
Mn II 257.6	0.012	0.023	0.21	1.9		18
Cr II 267.7	0.079	0.11	1.9	1.4		24
Mg II 279.5	0.0035	0.0053	0.093	1.5		27
Cd I 324.7	0.059	0.095	1.7	1.6		29
Pb II 220.3	0.50	0.70	16	1.4		32
Cd I 228.8	0.012	0.033	0.81	2.8		68
Average				1.8		39

system without a desolvation unit, the present thermospray/membrane system offers detection limits improved by on average a factor of 39 with a range from 18 to 68, which is in good agreement with the improvements in sensitivity as discussed in Section 3.4. Indeed, these values listed in the second column of Table 5 are very promising, and those for Mn, Mg, Cr and Cd are even comparable to the detection limits reported for pneumatic nebulization ICP mass spectrometry [41].

4. Conclusions

With ICP-AES and thermospray nebulization, the use of a multi-tube Nafion® membrane dryer as a secondary desolvation device enables a high desolvation efficiency for 1% (v/v) nitric acid and a low plasma solvent load, eliminates the need for a refrigerated recirculator for cooling the precondenser and allows more flexibility in choosing sweep gases than a porous membrane desolvator. The membrane was optimized at low temperatures and low sweep gas flow rates. Furthermore, the membrane was also shown to have a role as a pulse dampener. The vertical pulsation in the central channel of the plasma observed with thermospray nebulization was thus eliminated and the overall analytical performance of the system, including measurement precision and detection power, was significantly improved.

In addition to use with ICP-AES, the high desolvation efficiencies and pulse dampening capabilities

observed with this membrane dryer suggests that this system should also be useful with ICP mass spectrometry.

Acknowledgements

The authors would like to thank Perma Pure, Inc. for the loan of the Nafion® Membrane Dryer, Varian Instruments and Gerald Shkolnik for the Liberty 220 ICP spectrometer and Leeman Labs, Inc. and John Leeman for the thermospray nebulizer system used.

References

- [1] B.L. Gaughlin and M.W. Blades, *Spectrochim. Acta Part B*, 42 (1987) 353.
- [2] S.E. Long and R.F. Browner, *Spectrochim. Acta Part B*, 43 (1988) 1461.
- [3] S.E. Long and R.F. Browner, *Spectrochim. Acta Part B*, 41 (1986) 639.
- [4] J.W. Olesk, L.J. Smith and E.J. Williamson, *Anal. Chem.*, 61 (1989) 2002.
- [5] J.F. Adler, R.M. Bombelka and G.F. Kirkbright, *Spectrochim. Acta Part B*, 35 (1980) 163.
- [6] Y.Q. Tang and C. Trassy, *Spectrochim. Acta Part B*, 42 (1987) 353.
- [7] P.E. Walters and C.A. Barnard, *Spectrochim. Acta Part B*, 43 (1988) 325.
- [8] S. Nowak, J.A.M. van der Mullen, A.C.A.P. van Lammeren and D.C. Schram, *Spectrochim. Acta Part B*, 44 (1989) 411.
- [9] A. Canals, V. Hernandez, J.L. Todoli and R.F. Browner, *Spectrochim. Acta Part B*, 50 (1995) 305.

- [10] I.B. Brenner, J.M. Mermet, I. Segal and G.L. Long, *Spectrochim. Acta Part B*, 50 (1995) 323.
- [11] I.B. Brenner, I. Segal, M. Mermet and J.M. Mermet, *Spectrochim. Acta Part B*, 50 (1995) 333.
- [12] R.F. Browner, A. Canals and V. Heiniadis, *Spectrochim. Acta Part B*, 47 (1992) 659.
- [13] V.A. Fassel and B.R. Bear, *Spectrochim. Acta Part B*, 41 (1986) 1089.
- [14] S.K. Luo and H. Berndt, *Spectrochim. Acta Part B*, 49, (1994) 485.
- [15] N. Jakubowski, I. Feldmann, D. Stuewer and H. Berndt, *Spectrochim. Acta Part B*, 47 (1992) 119.
- [16] J.A. Koropchak and M. Veber, *Chit. Rev. Anal. Chem.*, 23 (1992) 113.
- [17] J.A. Koropchak and D.H. Winn, *Appl. Spectrosc.*, 41 (1987) 1311.
- [18] S. J. Hill, I. Hartley and L. Ebdon, *J. Anal. Atom. Spectrom.*, 7 (1992) 23 and 895.
- [19] D.R. Wiederin, R.S. Houk, R.K. Winge and A.P. D'Silva, *Anal. Chem.*, 62 (1990) 1155.
- [20] L.C. Alves, D.R. Wiederin and R.S. Houk, *Anal. Chem.*, 64 (1992) 1164.
- [21] L.C. Alves, L.A. Allen and R.S. Houk, *Anal. Chem.*, 65 (1993) 2468.
- [22] A. Montasser, H. Tan, I. Ishii, S.H. Nam and M. Cai, *Anal. Chem.*, 63 (1991) 2660.
- [23] M.A. Tarr, G. Zhu and R.F. Browner, *J. Anal. Atom. Spectrom.*, 7 (1992) 813.
- [24] K. Backstrom, A. Gustavsson and P. Hietala, *Spectrochim. Acta Part B*, 44 (1989) 1041.
- [25] A. Gustavsson and P. Hietala, *Spectrochim. Acta Part B*, 45 (1990) 1103.
- [26] J.W. McLaren and A. Gustavsson, *Spectrochim. Acta Part B*, 45 (1990) 1091.
- [27] H. Tao and A. Miyazaki, *J. Anal. Atom. Spectrom.*, 10 (1995) 1.
- [28] C. R. Blakely, J. J. Carmody and M. L. Vestal, *J. Amer. Chem. Soc.*, 102 (1980) 5931.
- [29] R.I. Boto and J.J. Zhu, *J. Anal. Chem. Spectrom.*, 9 (1994) 905.
- [30] N.G. Sundin, J.F. Tyson, G.P. Hanna, and S.A. McIntosh, *Spectrochim. Acta Part B*, 50 (1995) 369.
- [31] B.A. Fernandez, M.R. Fernandez de la Campa and A. Sanz-Medel, *J. Anal. Atom. Spectrom.*, 8 (1993) 1097.
- [32] W.T. Corns, L. Ebdon and S.J. Hill, *Analyst*, 117 (1992) 717.
- [33] T.S. Conner, S. McDaniel, J.A. Koropchak and D. Leighy, Presented at FACSS XXII, 15–20 October 1995, Cincinnati, OH, Paper 855.
- [34] T.S. Conner and J.A. Koropchak, *Spectrochim. Acta Part B*, 50 (1995) 341.
- [35] J.A. Koropchak, M. Veber and J. Henties, *Spectrochim. Acta Part B*, 47 (1992) 825.
- [36] D.D. Smith and R.F. Browner, *Anal. Chem.*, 54 (1982) 533.
- [37] Q. Jin, H. Zhang, Y. Wang, X. Yuan and W. Yang, *J. Anal. Atom. Spectrom.*, 9 (1994) 851.
- [38] H. Liu, T.S. Conner and J.A. Koropchak, presented at Pittsburgh Conference, 6–9 March 1995, New Orleans, LA, Paper 95F.
- [39] H. Liu and J.A. Koropchak, presented at FACSS XXII, 15–20 October 1995, Cincinnati, OH, Paper 735.
- [40] T.S. Conner, J. Yang, J.A. Koropchak, G. Shkolnik and C. Flajnik-Rivera, *J. Anal. Atom. Spectrom.*, accepted.
- [41] G. Horfick and Y. Shao, in A. Montasser and D. W. Golightly (Eds.), *Inductively Coupled Plasma in Analytical Atomic Spectrometry*, VCH, New York, 1992, Chapter 12.